J Electroceram (2011) 27:38–44
DOI 10.1007/s10832-011-9647-6

Extension sensing of piezo actuators using time-domain ultrasonic measurement and frequency-domain impedance measurement

Erman Uzgur · Shin-Sung Kim · Emma Bryce · David Hutson · Mel Strachan · Katherine J. Kirk

Received: 23 September 2008 / Accepted: 1 June 2011 / Published online: 18 June 2011
© Springer Science+Business Media, LLC 2011

Abstract There is a requirement for a simple and accurate extension sensing method for multilayer piezoelectric actuators for precision micro-positioning applications. This paper explains three different techniques of extension sensing for multilayer piezoelectric actuators, to provide a suitable method which involves primarily overcoming the inherent hysteretic behaviour of piezoelectric materials. The methods were; time domain ultrasonic pulse echo response for time travel of acoustic pulses, frequency shift response spectrum of an ultrasonic transducer and frequency shift in the impedance spectrum of the actuator alone. From the results, method of the frequency shift in the impedance spectrum of the actuator alone proved to be the most effective of the three. It was found that due to acoustic velocity changes under DC bias during the ultrasonic measurements, the inherent hysteretic behaviour was amplified in the other two methods when extension was plotted against time-shift and frequency shift. The results are presented and are discussed in terms of their suitability for precise positioning.

Keywords Extension sensing · Multilayer actuators · Self sensing · Ultrasound · Resonance spectrum

E. Uzgur (✉) · S.-S. Kim · E. Bryce · D. Hutson · K. J. Kirk
Microscale Sensors, School of Engineering, University of the West of Scotland,
Paisley, UK
e-mail: erman.uzgur@uws.ac.uk

M. Strachan
UK Astronomy Technology Centre, Royal Observatory,
Edinburgh, UK

1 Introduction

Piezoelectric materials are ideal for precision positioning for a number of applications including mirror positioning [1] and biological manipulation [2, 3]. However, piezoelectric materials exhibit fundamentally hysteretic behaviour in their response to an applied electric field and positioning precision can be significantly reduced due to this nonlinear effect. Thus, use of an extension sensor output is necessary to alleviate this problem and correctly control the actuator. While a number of techniques have been successfully used for actuator extension sensing based on capacitive, optical, and strain measurements [4–6], these techniques limit the miniaturization, complicate the system and increase the manufacturing cost. The simple integration of an extension sensor or use of self sensing actuators is highly desirable feature for many piezoelectric actuator applications [7–11].

This paper discusses three potential methods to overcome hysteresis by extension sensing of multilayer piezoelectric actuators. The reason multilayer piezoelectric actuators are used is that they are now the common within precise positioning applications. They provide increased displacement under low driving voltage compared to monolithic piezoelectric actuators. The three potential methods are outlined below.

When an ultrasonic pulse is transmitted from one end of the actuator, an echo is received due to a reflection from the other end. When the actuator is extended as a result of an applied DC bias, it is expected that the arrival time of the echo should change. Thus it could be expected that by measuring the time-shift of the ultrasonic echoes, the difference in the path-length of the ultrasound in the actuator can be deduced, and therefore the change of length of the actuator [12].

The resonant spectrum method has been widely used for the characterisation of piezoelectric films deposited on top of a substrate with known material parameters. When a piezoelectric transducer is attached on top of a piezoelectric actuator, the impedance spectrum of the transducer is superposed on the resonance spectrum of the actuator, with the superposed resonance peaks corresponding to integer multiples of the thickness of the actuator. Thus, the frequency shift of the resonance peaks could potentially be used as a measure of the changes in the thickness of actuator under DC bias [13, 14].

Use of the actuator for sensing as well as actuation has received great interest due to its advantages such as cost, simplicity and robustness [15–17]. The 'self-sensing' requires that there must be some measurable parameter of the actuator that can provide sensing information. We have investigated the possibility of using parts of the impedance spectrum of the actuator for extension sensing, with parameters of interest being the capacitance in the low frequency region and the zero-phase frequency in the capacitive-to-inductive transition region.

2 Experimental method

2.1 Time-domain pulse-echo method using ultrasonic transducer

For a time-domain pulse-echo measurement, a $7 \times 7 \times 2\,\text{mm}^3$ PZT-5A transducer having a fundamental resonance at 1.5 MHz was bonded to a $7 \times 7 \times 18\,\text{mm}^3$ multilayer piezo actuator (PI, P-887.51) with a fundamental resonance at 94 kHz. The actuator was connected to a DC voltage source and the transducer was connected to a pulser/receiver, through which the pulse-echo signal was monitored by an oscilloscope as shown in Fig. 1(a). The response of the echo signals for different applied voltages was recorded by computer control software. The shift in the arrival time of the echo was then calculated using cross-correlation of each echo with zero-bias echo signal.

2.2 Frequency-domain impedance method using transducer

The previous transducer was removed from the actuator and replaced by a 0.5 mm thick transducer with a fundamental resonance frequency of 4.5 MHz, for frequency-domain resonance spectrum measurements as shown in Fig. 1(b). The transducer was connected to an impedance analyser (Agilent 4294A). The change in its impedance, superimposed on resonances corresponding to the thickness mode of the underlying actuator, was measured for different values of DC bias.

2.3 Frequency-domain impedance method using actuator

The setup for impedance measurement of actuator under DC bias is shown in Fig. 1(c). A DC bias test fixture (Agilent 16065A) was required to prevent the DC voltage from influencing the impedance analyser. Two regions of the impedance spectrum of the actuator were investigated. The low-frequency region (~1 kHz) where the behaviour of the actuator can be approximated by a capacitor and the mid-frequency region (~300 kHz) where there is a sharp phase shift of the actuator impedance from capacitive to inductive. The gradient of the impedance magnitude vs. inverse frequency plot was estimated by linear regression and investigated as a measure of the extension of the actuator. The zero-phase frequency of the actuator at the phase shift was also related to the extension to investigate its usage as an indicator of the extension.

The actual extension of the actuator was simultaneously measured using an optical displacement sensor (MTI-2000 Fotonic™).

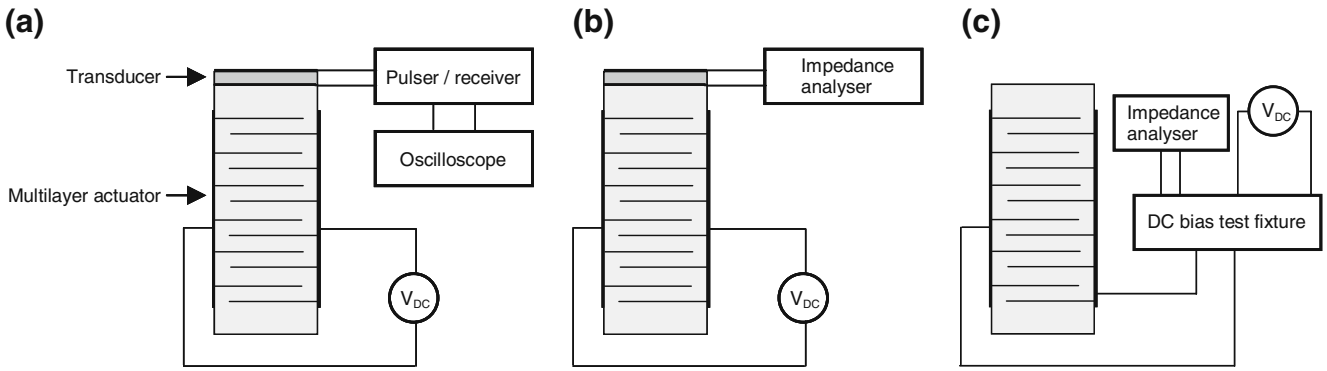

Fig. 1 Experimental setups for (**a**) pulse-echo measurement using bonded transducer on actuator, (**b**) resonant spectrum measurement using bonded transducer, and (**c**) impedance measurement of actuator under DC bias

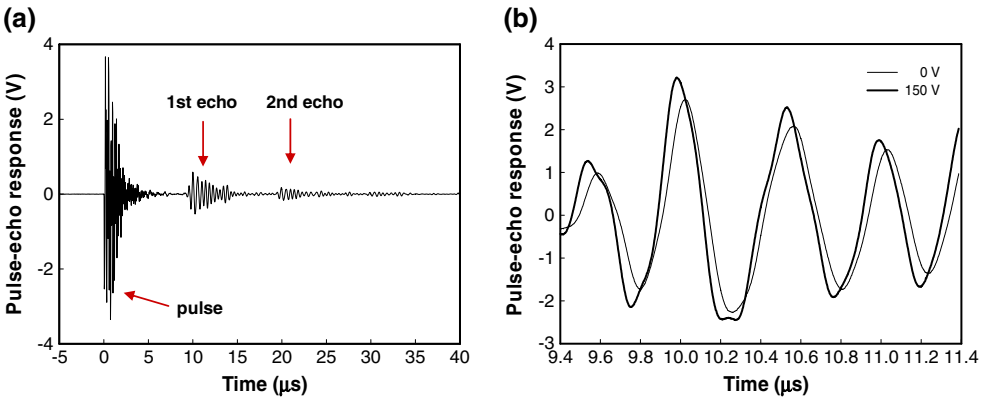

Fig. 2 (**a**) Pulse-echo response of actuator at 0 V and (**b**) echoes for 0 V and 150 V

3 Results

3.1 Time-domain pulse-echo method using transducer

The pulse-echo response of the actuator measured using the bonded transducer is shown in Fig. 2(a). A sequence of echoes was observed with around 9.25 μs intervals. The calculated velocity of ultrasound in the 18 mm thick actuator was 3,892 ms^{-1}. The first few periods in the first echo were monitored to see the effect of DC bias in the arrival time of the echo as shown in Fig. 2(b). A shift in the arrival time of the echo was observed as the DC bias was increased. The amount of time shift calculated by cross-correlation of the two signals was 29 ns. It should be noted that, contrary to simple intuition, an earlier arrival time of the echo is observed when the actuator is extended, suggesting an increased sound velocity under DC bias. Similar effects have been observed by others in the case of bulk PZT material, with increased resonance frequency shift for increased DC bias [18, 19]. However, our results provide a more direct and explicit manifestation of the phenomenon.

Figure 3(a) shows the actual displacement measured by the optical displacement sensor in terms of DC bias. The actuator exhibits an inherent hysteresis which is detrimental for precise position control. For an applied voltage of 60 V, one can expect 8.5±1.3 μm variation in the extension depending on the direction of voltage sweep. Figure 3(b) shows time shift of the echo in terms of voltage. The reading at 60 V is −9±7.0 ns. The apparent amplification of

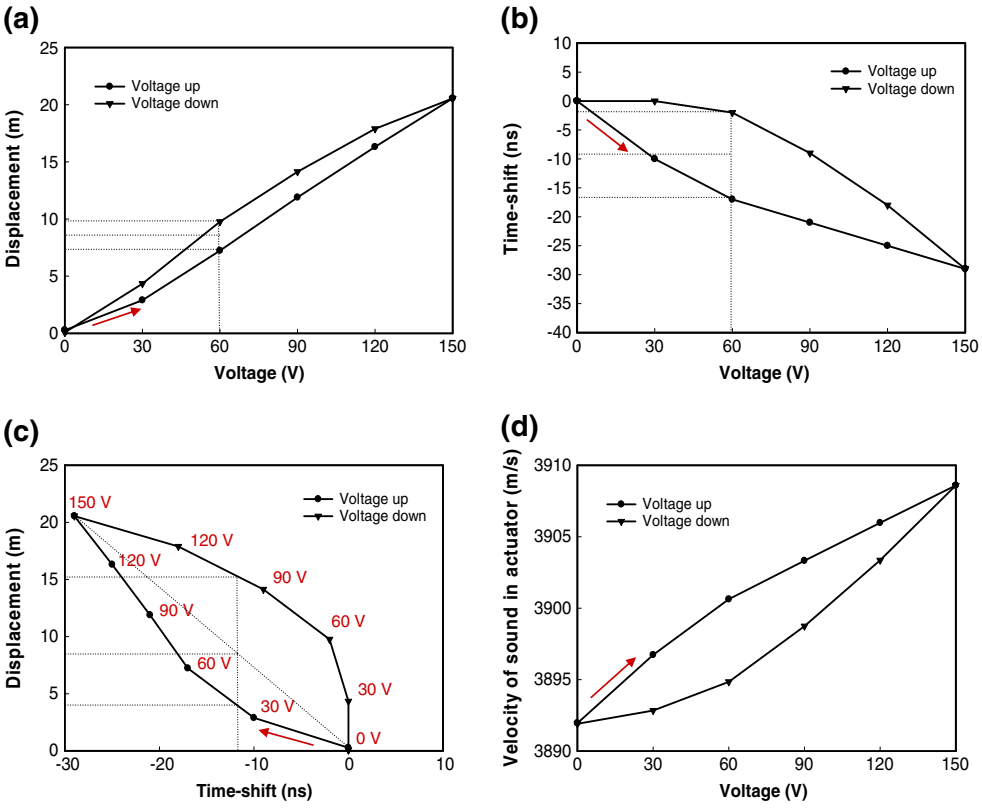

Fig. 3 Bias-dependent characteristics of the actuator: (**a**) extension (**b**) time shift of echo arrival time (**c**) extension vs time shift and (**d**) ultrasonic velocity in the actuator

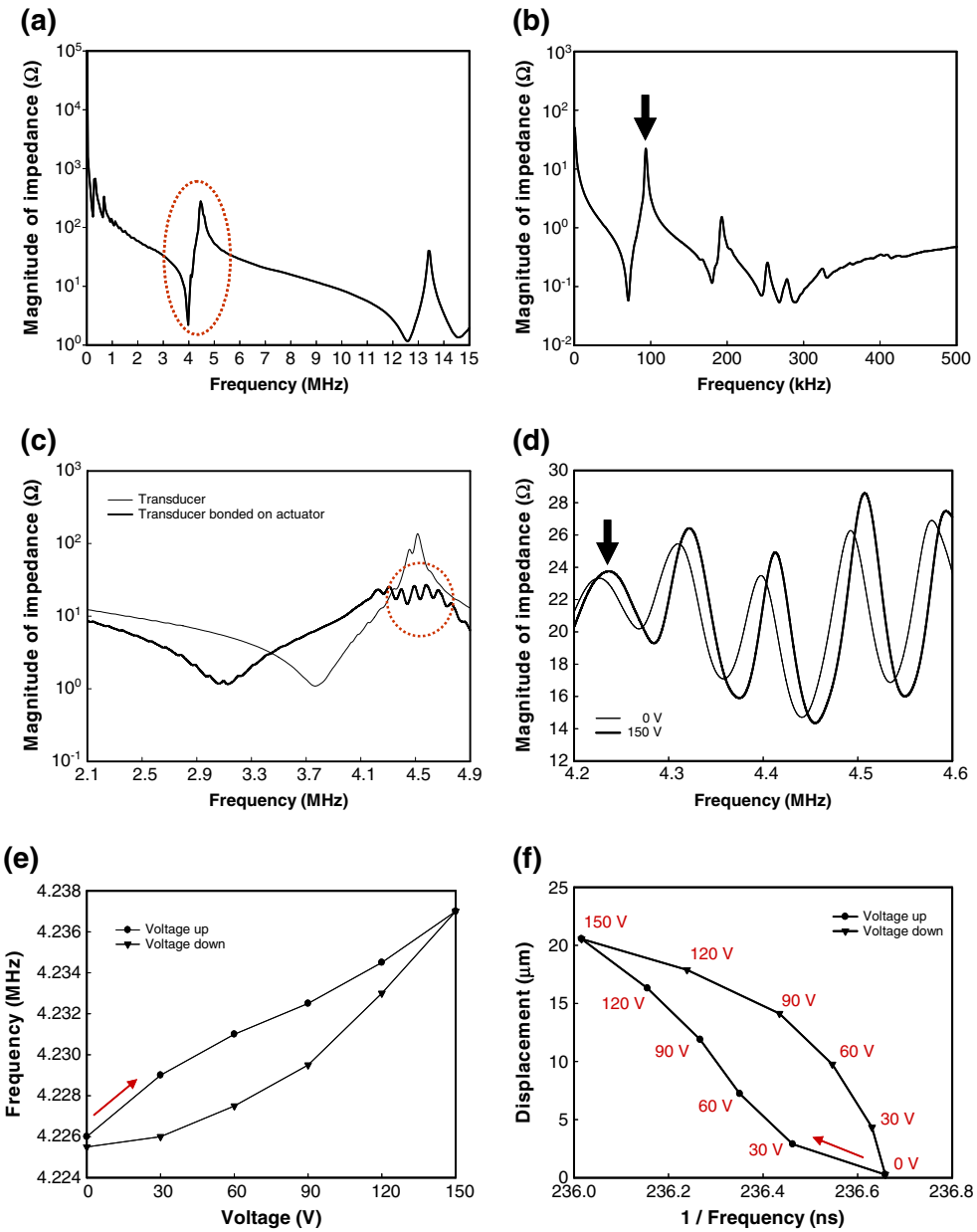

Fig. 4 (**a**) Impedance of $7 \times 7 \times 0.5\,\text{mm}^3$ PZT-5A transducer, (**b**) impedance of $7 \times 7 \times 18\,\text{mm}^3$ actuator, (**c**) impedance of transducer before and after bonding on to the actuator (enlarged view of the area in (**a**) *marked by a circle*), (**d**) shift of overtones under DC bias (enlarged view of the area in (**c**) *marked by a circle*), (**e**) resonance frequency, indicated by an *arrow* in (**d**), in terms of DC bias, and (**f**) extension vs inverse frequency

the hysteresis in the time shift seems to be a detrimental feature when it is to be used to measure the extension. The problem can be better understood in the plot of extension against time shift as in Fig. 3(c). When an extension of 8.5 μm is aimed at using the time shift, one can expect an extension error between +6.7 and −4.5 μm, which corresponds about 66% of the extension range.

While extension sensing using the time-shift of echo does not seem to be an attractive option when used in this way, it can be a very useful tool for the characterising the ultrasonic velocity in the actuator and its behaviour under DC bias as shown in Fig. 3(d). The ultrasonic velocity increases as the voltage increases, with a 0.4% increment from 0 V to 150 V. Note that the velocity is higher during the upward voltage sweep than for the downward sweep.

3.2 Frequency-domain impedance method using transducer

The impedance spectrum (magnitude and phase) of the transducer $(7 \times 7 \times 0.5\,\text{mm}^3)$ and the actuator $(7 \times 7 \times 18\,\text{mm}^3)$ used in the resonance spectrum experiment were measured separately before bonding as shown in Fig. 4(a) and (b). The fundamental resonance of the transducer and the actuator occur at approximately 4.5 MHz and 94 kHz, respectively. The impedance spectra of the transducer before and after bonding are shown in Fig. 4(c), which is an enlarged view of the circled area in Fig. 4(a). It is evident that the bonding of actuator introduces superposed resonances to the original spectrum. Figure 4(d) is an enlarged view of the area where these resonances are most pronounced, corresponding to the circled area in Fig. 4(c).

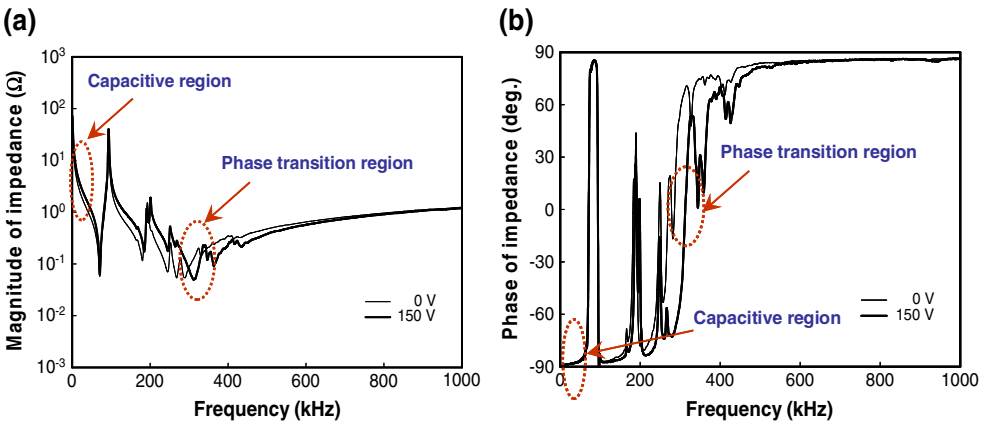

Fig. 5 The impedance of 7 × 7 × 18 mm^3 actuator under DC bias: (**a**) magnitude and (**b**) phase

The spacing between adjacent resonance peaks was approximately 108 kHz, and is close to the value obtained from a simple calculation of the longitudinal mode resonance of 94 kHz. As the DC bias increased to 150 V the resonant peaks relating to the actuator all shift towards higher frequencies. The shift of the peak indicated by an arrow in Fig. 4(b) in terms of different applied voltages is shown in Fig. 4(e), where it can be seen that the shape is very similar to the curve of extension against time-shift shown in Fig. 3(b). When the extension is plotted against the inverse frequency (which has a unit of time), as in Fig. 4(f), the curve exhibits a marked resemblance to the result from pulse-echo as shown in Fig. 3(c). These results suggest that we are measuring the same effect in both time-domain and frequency-domain. The conforming results from both domains help to validate our ultrasonic extension sensing techniques.

3.3 Frequency-domain impedance method using actuator

The impedance phase and magnitude of the 7 × 7 × 18 mm^3 multilayer actuator under 0 V and 150 V bias are shown in Fig. 5(a) and (b). The two characteristic regions marked by red circles are the capacitive region (<50 kHz) and the phase transition region (~300 kHz). These regions were chosen because of the explicit relevance of the extension to the capacitance of actuator due to the increased separation of internal electrodes and because of the large frequency shift observed in the frequency of the phase transition under DC bias.

The magnitude of impedance when plotted in terms of inverse frequency shows a linear relationship as in Fig. 6 (a). The gradient of the plot, *m*, is proportional to the inverse capacitance and hence is related to the extension. The calculated capacitances from the slope are 3.20 μF for 0 V and 2.22 μF for 150 V. The actual extension in terms of *m* is shown in Fig. 6(b), in which the degree of hysteresis is much reduced compared to those in Figs. 3(c) and 4(f), based on the pulse-echo method and the resonance spectrum method, respectively. For a target extension of 8.5 μm based on the reading of *m*, one can now expect an uncertainty in the extension of ±0.6 μm.

Another part of the impedance spectra of the actuator that gives a noticeably measurable change in response to applied voltage is the region around 300 kHz, where a marked phase transition from capacitive to inductive behaviour occurs. The zero-phase point in that region

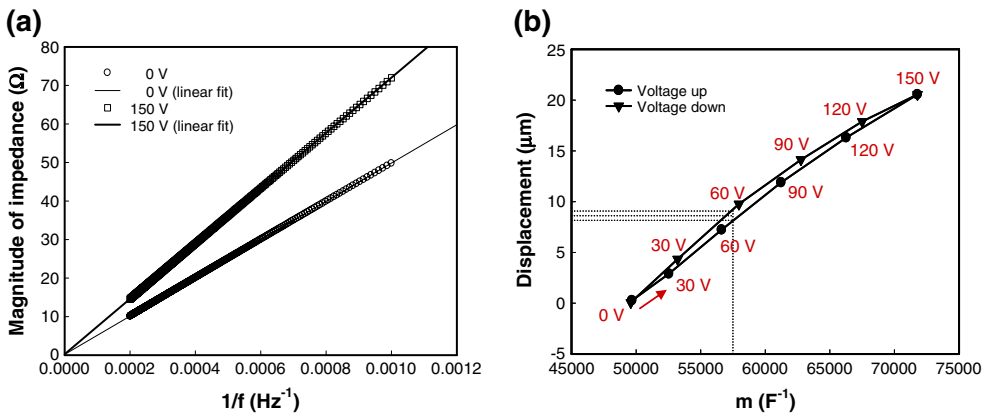

Fig. 6 The characteristics of 7 × 7 × 18 mm^3 actuator under DC bias in capacitive region: (**a**) magnitude of impedance vs inverse frequency and (**b**) actual extension vs *m*

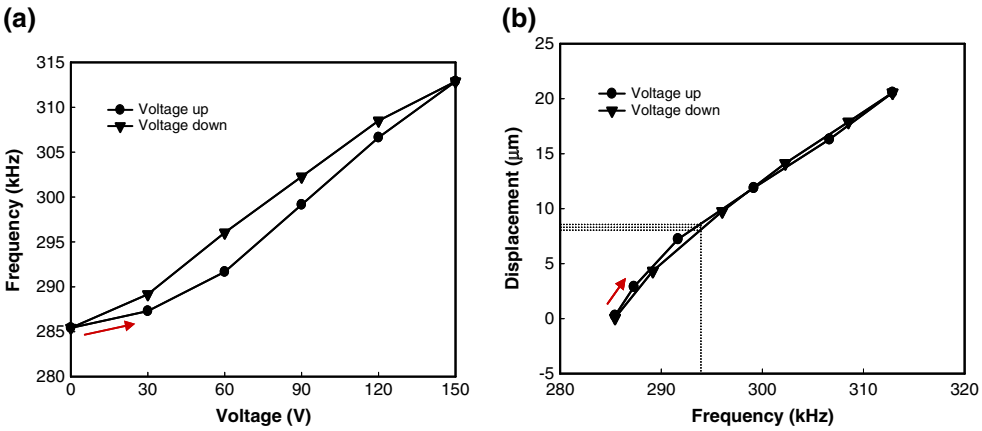

Fig. 7 The characteristics of $7 \times 7 \times 18\,mm^3$ actuator under DC bias in phase transition region: (**a**) zero-phase frequency vs voltage and (**b**) actual extension vs zero-phase frequency

moves towards higher frequency as the voltage increases as shown in Fig. 7(a).The shape of the hysteresis loop is very similar to that for actuator extension shown in Fig. 3(a). As a result, the actual extension in terms of the frequency shift shows a significant decrease in the amount of hysteresis as well as an improved linearity as shown in Fig. 7(b). For a target extension of 8.5 μm based on the reading of the zero-phase frequency, one can now expect an extension error of ±0.4 μm.

4 Discussion

The pulse-echo method and the resonance spectrum method using piezoelectric transducer promised to be a viable means of extension sensing. The sensing principles based on both methods are in principle relatively simple. However, complications arose due to the sound velocity changes in the actuator material under DC bias: faster sound velocity for higher voltage. As a result, the inherent hysteretic behaviour in the extension of actuator was amplified in the extension plotted against time-shift and the frequency shift. The physics behind the phenomenon is being investigated but we believe the complication arises from domain movement in PZT.

The impedance spectrum of a multilayer piezoelectric actuator contains useful pieces of information on its electrical and mechanical behaviour, which, with proper manipulation, might be used for extension sensing. The interpretation of the impedance spectra for multilayer actuators, however, is not as straightforward as for single layer electric resonators due to their relatively complex structures. The approximation of multilayer actuators at low frequency by a single value of capacitance can easily accepted, however the dependence of the frequency of the phase transition between capacitive and inductive behaviour currently escapes a ready explanation. Further investigation is required to understand the observed capacitive-to-inductive phase transition in the impedance and its shift in response to DC bias.

5 Conclusions

Three different techniques of actuator extension sensing have been demonstrated for a $7 \times 7 \times 18\,mm^3$ multilayer piezoelectric actuator and comparison was made in terms of their hysteretic behaviour. The pulse-echo and resonant spectrum techniques using an ultrasonic transducer provide a useful tool for the observation of faster sound velocity in the actuators under bias although can amplify hysteresis under certain conditions. Use of the impedance of actuator in capacitive and phase-transition regions proved to be a viable extension sensing technique, outperforming other techniques in providing an accurate indication of the actuator extension. In particular, the phase transition frequency of actuator showed the best extension sensing capability, which gives an uncertainty in the extension of ±0.4 μm for a target extension of 8.5 μm.

Acknowledgements The authors would like to thank Gerry O'Hare, Technician, for his work within the laboratory.

References

1. Using piezo to probe the secrets of the universe, Piezo-News, Newsletter of Piezo Institute, Issue 4, 2009
2. H.C. Liaw, B. Shirinzadeh, Sens. Actuators A **147**, 254 (2008)
3. K.K. Tan, S.C. Ng, Eng. Sci. Educ. J. **10**, 249 (2001)
4. T. Schmitza, K. Prumea, B. Reichenberga, A. Roelofsb, R. Waserb, S. Tiedkea, J. Eur. Ceram. Soc. **24**, 1145 (2004)
5. Y.B. Dong, V.E. Zubov, A.D. Kudakov, J. Magn. Magn. Mater. **160**, 157 (1996)

6. C. Pientschke, A. Kuvatov, R. Steinhausen, H. Beige, R. Krüger, T. Müller, U. Helbig, D. Sporn, C. Schuh, S. Denneler, T. Richter, H. Schlich, J. Eur. Ceram. Soc. **29**, 1713 (2009)
7. X. Xu, Y. Feng, B. Li, J. Chu, Sens. Actuators, A **147**, 242 (2008)
8. J. Dong, P.M. Ferreira, J. Micromechanics Microengineering **18**, 035011 (2008)
9. L.L. Chu, Y.B. Gianchandani, J. Micromechanics Microengineering **13**, 279 (2003)
10. G.E. Simmers, J.R. Hodgkins, D.D. Mascarenas, G. Park, H. Sohn, J. Intell. Mater. Syst. Struct. **15**, 941 (2004)
11. S. Kim, E. Uzgur, M. Strachan, J.F. Saillant, K. Kirk, Adv. Sci. Tech. **56**, 70 (2009)
12. D.K. Hsu, M.S. Hughes, J. Acoust. Soc. Am. **2**, 669 (1992)
13. Y. Zhang, Z. Wang, J. David, N. Cheeke, IEEE Trans. Ultrason. Ferroelectr. Freq. Control **50**, 321 (2003)
14. M. Al Ahmad, H.N. Alshareef, Electrochem. Solid-State Lett. **13**, G108 (2010)
15. S. Wu, S. Mo, B. Wu, Sens. Actuators, A, Phys. **141**, 558 (2008)
16. K. Kuhnen, M. Schommer, H. Janocha, Smart Mater. Struct. **16**, 1098 (2007)
17. Y. Ishikiriyama, T. Morita, JAMDSM **4**, 143 (2010)
18. Q. Wang, T. Zhang, Q. Chena, X. Dub, Sens. Actuators, A, Phys. **109**, 149 (2003)
19. T. Kobayashi, R. Maeda, T. Itoh, J. Micromechanics Microengineering **18**, 03525 (2008)